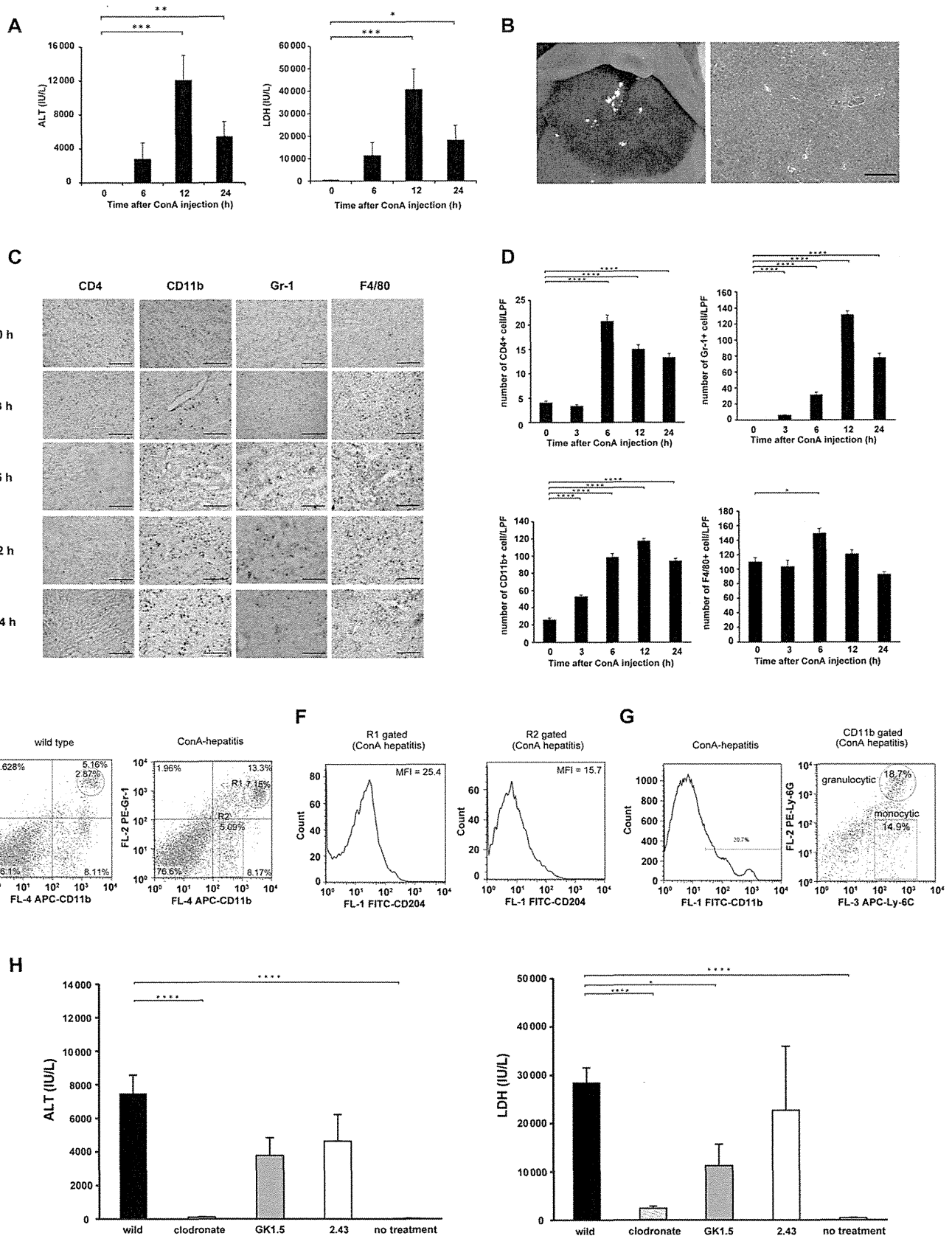

appearance of the liver obtained from mice injected with 300 μg of ConA followed by ADSC administration showed a mild and spotty white area with an almost normal color (Fig. 3C). Liver histology showed an almost normal appearance, with no necrosis (Fig. 3C), indicating that ConA-induced hepatitis was markedly ameliorated by ADSC treatment. No preventive or therapeutic effect on ConA-induced hepatitis resulted from administration of primary cultured murine hepatocytes ($n = 3$); there was no significant reduction in serum ALT or LDH (Fig. 3A and B), macroscopic necrosis appearance, or histological necrosis, compared with ConA-induced hepatitis (Fig. 3C).

ADSC treatment reduces elevated cytokine/chemokine concentrations in ConA-induced hepatitis mice

Marked protective and therapeutic effects of ADSCs on ConA-induced hepatitis were observed. To determine the effect of ADSC treatment on systemic inflammation in ConA-induced hepatitis, we measured serum cytokine and chemokine concentrations in ConA-induced hepatitis mice treated with ADSCs. Mice injected with ConA were immediately treated with ADSCs and serum was collected 6 h after ConA injection ($n = 3$). The elevated serum IFN-γ, IL-2, IL-6, IL-4, IP-10, MIG, KC, and MCP-1 levels in ConA-injected mice ($n = 3$) were significantly reduced by ADSC treatment (Supporting Information Fig. 1A). Injection of mice with ADSCs 3 h after ConA administration ($n = 4$) resulted in significantly reduced serum IFN-γ, IL-2, IL-6, and MIG levels, compared to ConA-injected mice not treated with ADSCs ($n = 6$) (Supporting Information Fig. 1B). Thus, the levels of the array of cytokines and chemokines that are elevated in the sera of ConA-induced hepatitis mice were significantly decreased by ADSC treatment.

Distribution of i.v. administered ADSCs in ConA-induced hepatitis murine models

The distribution of administered ADSCs in ConA-induced hepatitis mice was determined by immunohistochemistry. Administered GFP-expressing ADSCs were observed in the lung, but not the liver, of mice injected with ConA followed by immediate ADSC administration ($n = 6$), through 24 h (Supporting Information Fig. 2A). When administered to mice 3 h after ConA injection ($n = 6$), GFP-expressing ADSCs were observed primarily in the lung, and a few in the liver (Supporting Information Fig. 2B), suggesting that some fraction of ADSCs reached the liver upon occurrence of hepatitis.

Hepatic gene expression changes by ADSCs treatment are associated with Gr-1$^+$ and CD11b$^+$ cells

To investigate the detailed biological features of the liver in ConA-induced hepatitis mice that were treated with ADSCs, we examined the gene expression profiles of liver tissue of ConA-injected mice obtained 2 h after treatment with ADSCs using a DNA microarray. In the liver tissues of mice treated with ADSCs immediately after ConA injection ($n = 3$), 589 gene probes were differentially expressed compared with that in mice with ConA-induced hepatitis that had not been treated with ADSCs ($n = 3$). Expression of the majority of genes was downregulated by ADSCs, as shown by green color ($p < 0.05$; Fig. 4A). Principal component analysis using these genes showed a discernible distribution difference between the ADSC-treated and -untreated groups (Fig. 4B). When mice received ADSC treatment 3 h after ConA injection, hepatic expression of 309 gene probes was altered significantly compared with those in mice with ConA-induced hepatitis that had not been treated with ADSCs ($n = 3$). Expression of the majority of genes was downregulated by ADSCs, as shown by green color ($p < 0.01$; Fig. 4C). Principal component analysis of these genes also showed a discernible distribution difference between the ADSC-treated and untreated groups (Fig. 4D). In the context of biological maps of the genes affected by immediate ADSC treatment, cell differentiation, the inflammatory response, the DNA damage response, and apoptosis predominated (Supporting Information Table 1). In addition to these maps, tissue remodeling and wound repair, mitogenic signaling, and vascular development (angiogenesis) predominated in mice that had received ADSC treatment 3 h after ConA injection (Table 1), indicating that ADSCs provided not only anti-inflammatory effects, but also remodeling effects, in the ConA-damaged liver.

◀ **Figure 1.** Characteristics of ConA-induced hepatitis in C57BL/6 mice. (A–D) C57BL/6 female mice were injected i.v. with 300 μg of ConA. Sera and liver tissues were obtained 3, 6, 12, and 24 h after ConA injection. The data are representative of three individual experiments. (A) ALT and LDH activity in sera. Results are expressed as means ± SE ($n = 4$). $^*p < 0.05$, $^{**}p < 0.01$, $^{***}p < 0.005$ versus 0 h (Student's *t*-test). (B) Representative liver tissues obtained 12 h after ConA injection were assessed macroscopically and microscopically. Magnification: ×100. Bar: 200 μm. (C) Immunohistochemical staining for CD4, CD11b, Gr-1, and F4/80 in the livers of mice for each time point (0, 3, 6, 12, and 24 h; $n = 4$ per time point). Representative images of mice for each time point are shown. Magnification: ×100. Bar: 200 μm. (D) Quantification of the number of CD4$^+$, CD11b$^+$, Gr-1$^+$, and F4/80$^+$ cells in four visual fields per ×100 low-power field in the livers of representative mice in each group. Magnification: ×100. $^*p < 0.05$, $^{****}p < 0.001$ versus untreated mice (Student's *t*-test). (E–G) Hepatic inflammatory cells were isolated from mice 6 h after ConA injection, incubated with fluorescence-conjugated antibodies, and assessed by FACS. Three mice per group per experiment. Experiments were performed twice. (E) Frequency of CD11b$^+$Gr-1$^+$ cells in WT C57BL/6 mice and ConA hepatitis mice. (F) Analysis of CD204 expression in CD11b$^+$Gr-1$^+$ cells (R1-gated region in (E)) and CD11b$^+$Gr-1$^-$ cells (R2-gated region in (E)) among hepatic inflammatory cells from ConA hepatitis mice. MFI: mean fluorescence intensity. (G) CD11b$^+$ cells among hepatic inflammatory cells from ConA hepatitis mouse were gated, and Ly-6C and Ly-6G expression levels in the gated cells were determined. (H) C57BL/6 female mice were injected i.v. with clodronate ($n = 4$), i.p. with anti-CD4 antibody (GK1.5) ($n = 4$), or anti-CD8 antibody (2.43) ($n = 4$) every 24 h for 2 days. The mice were then injected i.v. with 300 μg of ConA. Sera were obtained 24 h after ConA injection, and ALT and LDH activities were then measured. Results are expressed as means +SE ($n = 4$ per group) and are representative of one experiment performed. $^*p < 0.05$, $^{****}p < 0.001$ versus ConA-injected WT mice ($n = 4$) (Student's *t*-test).

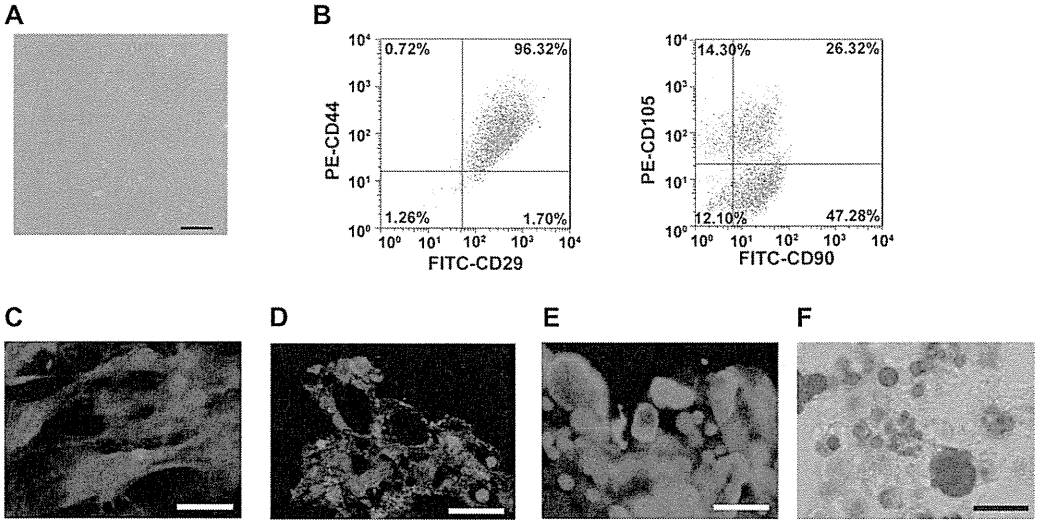

Figure 2. Characteristics and pluripotency of cultured ADSCs. Cells in the stromal fraction of adipose tissues from mice were cultured, maintained, and expanded for eight to ten passages. (A) Spindle shaped cells were observed after eight passages. Magnification: ×100. Bar: 200 μm. (B) Flow cytometric analysis of CD29, CD44, CD90, and CD105 surface marker expression. The data shown are representative of three independent experiments. (C–F) ADSCs were cultured with specific growth factors for induction of osteocytes, chondrocytes, and adipocytes using a mouse mesenchymal stem cell functional kit. Immunohistochemical staining was performed with (C) anti-osteopontin antibody for osteocytes, (D) anti-collagen II antibody for chondrocytes, and (E) anti-FABP antibody as well as (F) Oil-Red O staining for adipocytes. Magnification: x200. Bars: 50 μm. All data shown are from one experiment representative of two independent experiments performed.

Next, we investigated the relevance of these altered genes in the context of inflammatory cells using the public gene expression database of hematopoietic cells and stem cells (GSE27787). The annotated genes among the 589 gene probes detected by microarray analysis probes in the livers of mice that received ADSC treatment immediately after ConA injection were not relevant to any hematopoietic cell type (Fig. 4E). By contrast, among the 309 gene probes, the majority of the annotated genes whose hepatic expression in mice that received ADSC treatment 3 h after ConA injection was affected significantly were found to be highly expressed in Gr-1$^+$ cells and Mac1$^+$ (CD11b$^+$) cells — as indicated by the red color (Fig. 4F). Since majority of the 309 gene probes in the liver of ConA hepatitis were downregulated by ADSC treatment, as indicated by green color (Fig. 4C), these results suggested that effects on Gr-1$^+$ and CD11b$^+$ cells were associated with the therapeutic effect of ADSCs 3 h after ConA injection.

ADSC treatment represses inflammatory cell accumulation in ConA-induced hepatitis

To determine the influence of ADSC treatment on the infiltration/accumulation of immune-mediating cells in the liver of ConA-induced hepatitis mice, we assessed by immunohistochemistry the inflammatory cells in the liver tissues of mice injected with ConA followed by ADSC administration at 3 h. Liver tissues obtained at 6, 12, and 24 h ($n = 4$ each time point) after ConA injection showed reduced accumulation of CD11b$^+$ cells, Gr-1$^+$ cells, and F4/80$^+$ cells after ADSC treatment (Fig. 5). In contrast, the increased number of infiltrated CD4$^+$ T cells in ConA-induced hepatitis mice was not significantly affected by the ADSCs (Fig. 5). Thus, the predominant change in ConA-induced hepatitis mice treated with ADSCs was in the number of myeloid-lineage inflammatory cells, consistent with the hepatic gene expression data.

T-cell involvement in the altered gene expression of hepatic inflammatory cells by ADSCs treatment

To further assess the anti-inflammatory effects of ADSCs in mice with ConA-induced hepatitis, we isolated hepatic inflammatory cells from mice 2 h after ADSC treatment, which was administered 3 h after ConA injection ($n = 2$) and from mice not treated with ADSCs ($n = 2$). A total of 939 genes were differentially expressed in hepatic inflammatory cells from ConA-induced hepatitis mice treated with ADSCs. The gene expression profiles associated with ADSC treatment and ConA-induced hepatitis without ADSC treatment were readily distinguishable (Supporting Information Fig. 3A). Pathway map analysis showed that these genes were relevant to biological pathways of oncostatin M signaling via JAK-Stat or MAPK signaling and CCR5 signaling in macrophages and T lymphocytes in the immune response pathway (Supporting Information Table 2). Network analysis of these genes featured a network consisting of AcRIIA, STAT3, Activin A, FTSJD1, and STAT1 at the top (Supporting Information Table 3), which indicated that pathways involving IL-2 and TNF-α, and the STAT1/STAT3 pathway were also involved (Supporting Information Fig. 3B). These results suggest that T cells, as well as antigen presenting/phagocytosis lineages, were the immune-mediating cell populations affected by ADSC treatment.

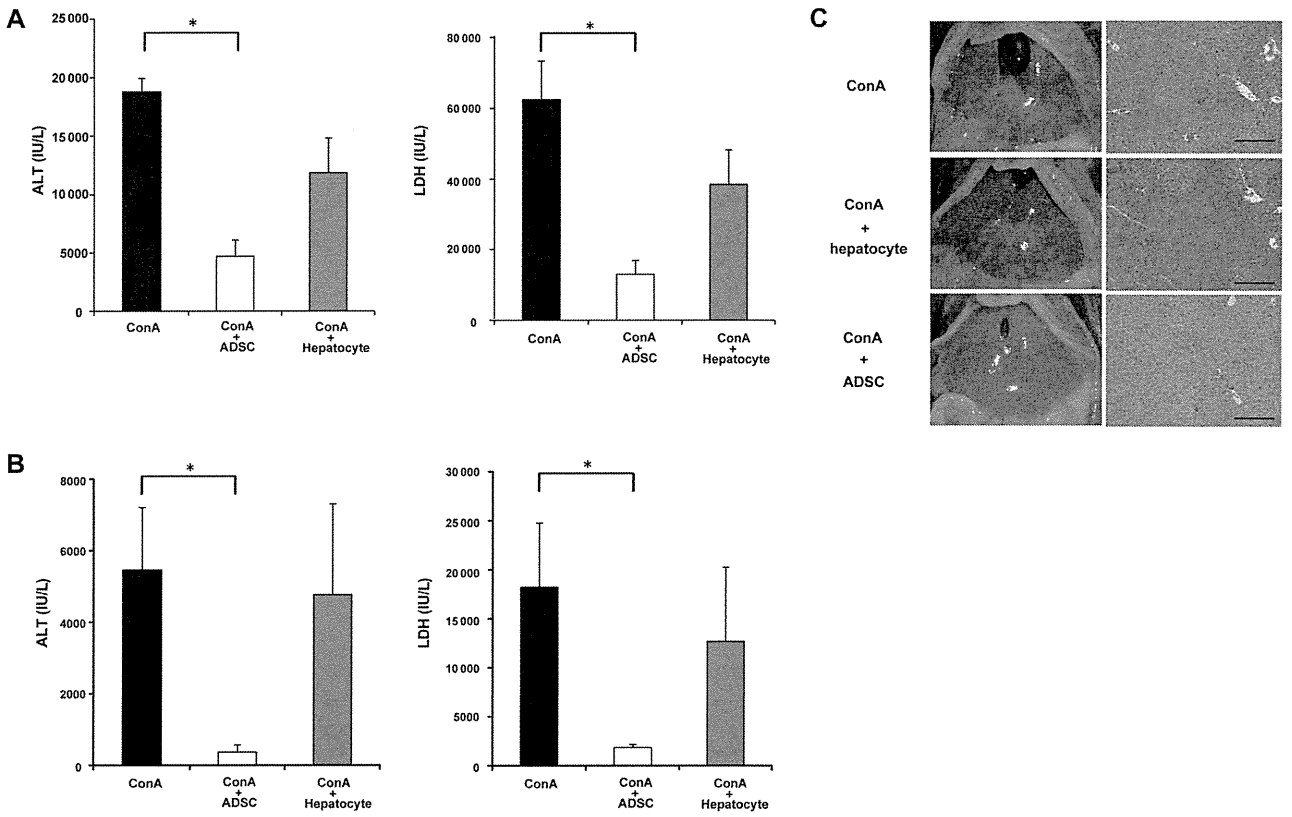

Figure 3. Therapeutic effects of ADSCs in ConA-induced hepatitis. C57BL/6 female mice were injected i.v. with 300 μg of ConA. Immediately or 3 h later, 1×10^5 ADSCs or hepatocytes were injected via the tail vein. Liver tissues and blood samples were obtained 24 h after ConA injection. Liver tissues were examined histologically and serum ALT and LDH activities were measured. (A, B) Serum ALT and LDH activities of mice injected with ConA followed by ADSC injection (A) immediately or (B) 3 h later. ConA: ConA-injected mice without treatment ($n = 4$), ConA + ADSC: ConA-injected mice followed by ADSC treatment ($n = 3$), ConA + hepatocyte: ConA-injected mice followed by primary cultured hepatocyte treatment ($n = 3$). Data are shown as mean ± SE and are from one experiment representative of two independent experiments. *$p < 0.05$ (Wilcoxon signed-rank test), compared with ConA-injected mice. (C) Macroscopic appearance of the liver (left) and histology of the liver tissues as assessed by H&E staining (right). Magnification of histology: ×100. Bars: 200 μm. Images shown are from one mouse representative of three to four mice from each group studied.

ConA-activated CD4$^+$T cells and CD11b$^+$ cells in the liver are important targets of ADSC treatment

The above data indicated that ADSCs administered in ConA-induced hepatitis had therapeutic immunological effects in terms of repairing the damaged liver and affected CD11b$^+$ and Gr-1$^+$ myeloid-lineage cells and T cells. To further explore how ADSCs affected the subpopulations of inflammatory cells involved in ConA-induced hepatitis, we investigated the expression of cytokine/chemokine-related genes in CD4$^+$ T cells and CD11b$^+$ cells obtained from livers with ConA-induced hepatitis ($n = 4$) that had been treated in vitro with ADSCs ($n = 3$). Expression of TNF-α, IL-10, and CXCL10 was significantly downregulated by ADSC treatment in both CD4$^+$ T cells (Supporting Information Fig. 4A) and CD11b$^+$ cells (Supporting Information Fig. 4B). IFN-γ, IL-4, and CXCL9 expression by CD4$^+$ T cells were significantly affected by ADSCs. Although CCL3, which was upregulated by ConA injection, was not significantly affected by ADSCs, the expression of its cognate receptor, CCR5, was decreased in CD4$^+$ T cells (Supporting Information Fig. 4A), suggesting an effect on the CCL3-CCR5 axis. These results suggest that CD4$^+$ T cells and myeloid-lineage CD11b$^+$ cells were the susceptible hepatic inflammatory subpopulations of cells in the ConA-induced hepatitis liver.

Anti-inflammatory effect of ADSCs on ConA hepatitis do not rely on MDSCs

We further assessed whether the anti-inflammatory effect of ADSCs in ConA hepatitis relied on MDSCs. Neither the frequency of nor the NO production by CD11b$^+$Gr-1$^+$ cells were increased by ADSC treatment (Supporting Information Fig. 5A). CD11b$^+$Gr-1$^+$ cells from ConA-injected mice treated with ADSCs showed arginase activity similar to that in CD11b$^+$Gr-1$^+$ cells from ConA-injected mice (Supporting Information Fig. 5B). CD11b$^+$Gr-1$^+$ cells from ConA-injected mice treated with ADSCs suppressed the ConA-stimulated proliferation of T cells in vitro, although the effect was slightly attenuated compared to that of cells from mice with ConA-induced hepatitis (Supporting Information Fig. 5C). Thus, ADSC treatment was not dependent on MDSCs induced by ConA hepatitis.

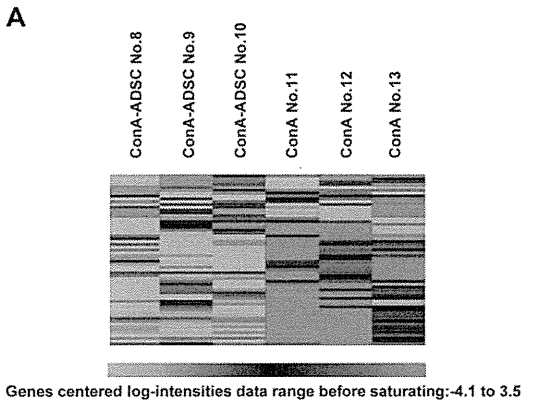

Discussion

MSCs are effective for immune-mediated disease treatment including the ConA-induced BALB/c murine hepatitis model [15], but the detailed mechanisms have not been fully elucidated. Here, we confirmed that ADSCs have preventive and therapeutic effects in a ConA-induced C57BL/6 hepatitis murine model and assessed the immunopathological mechanisms by determining the participating hepatic immunomodulatory cells. ADSCs injected via the tail vein were found in the lung; some were observed in the liver but only when ADSCs were administered 3 h after ConA injection, a time at which infiltration of $CD11b^+$ and $Gr\text{-}1^+$ inflammatory cells into the liver had already begun. Gene expression analysis of liver tissue from ConA-induced hepatitis mice showed that the ADSC treatment induced biological pathways indicative of liver repair and regeneration. Myeloid-lineage cells were the predominant population in terms of affected genes, consistent with immunohistochemical staining of the liver for immune-mediating cells. Furthermore, the gene expression profiles of hepatic inflammatory cells from ConA-induced hepatitis mice treated with ADSCs suggested T-cell and macrophage involvement. Moreover, the expression patterns of cytokine/chemokine-related genes in hepatic inflammatory cells co-cultured with ADSCs suggested that $CD4^+$ T cells were important in ConA-induced hepatitis and were affected by ADSC treatment.

The immunopathological features of ConA-induced hepatitis have been characterized as being primarily lymphocyte-lineage cell-mediated hepatitis [18–20], leading to massive hepatocellular degeneration, necrosis, and apoptosis [21]; thus, this model is relevant to clinical autoimmune hepatitis. Additionally, Kupffer cells play an important role in induction of hepatitis [22]. Unexpectedly, we observed prominent increases in $CD11b^+$, $Gr\text{-}1^+$, and $F4/80^+$ cells in liver tissues of the ConA-induced hepatitis mice. Additionally, we found that the monocyte-macrophage lineage cells contributed most significantly to hepatitis, as confirmed by depletion treatment, such that hepatitis was almost completely abolished when those cell types were abrogated by clodronate. This is further evidenced by the fact that ADSC treatment reduced the number of $CD11b^+$, $Gr\text{-}1^+$, and $F4/80^+$ cells in the liver of ConA-induced hepatitis mice (Fig. 5). The importance of $Gr\text{-}1^+$ and $CD11b^+$ cells was also suggested by changes in the gene expression profile of the liver of ConA-induced hepatitis treated with ADSCs (Fig. 4C and F). Thus, monocyte-macrophage lineage cells are important in the pathogenesis of ConA-induced hepatitis in mice and are important targets of ADSCs. $CD4^+$ T cells were also involved since their depletion partially ameliorated ConA-induced hepatitis. The number of infiltrating $CD4^+$ T cells in the liver of ConA-induced hepatitis mice was not markedly reduced by ADSC treatment. However, gene expression analysis of hepatic inflammatory cells in ConA-induced hepatitis mice treated with ADSCs showed that signaling of oncostatin M, a type I cytokine associated with developing T cells [23], and CCR5 signaling in macrophages and T lymphocytes were affected. Therefore, $CD4^+$ T cells participate as an immune mediator and therapeutic target of ADSCs in the pathology of ConA-induced hepatitis mice.

With regard to cytokine/chemokine-related gene expression in hepatic inflammatory cells of ConA-induced hepatitis mice, expression of TNF-α, IL-10, and CXCL10 in $CD4^+$ T cells and $CD11b^+$ cells was downregulated by ADSC treatment (Supporting Information Fig. 4). Additionally, IFN-γ, IL-4, and CXCL9 were also significantly downregulated in $CD4^+$ T cells, but not in $CD11b^+$ cells (Supporting Information Fig. 4). Changes in the expression of the Th2 cytokines, IL-10 and IL-4, were considered to be the secondary consequence of ConA-induced hepatitis, mediated by TNF-α and/or IFN-γ, which are characterized as Th1-associated cytokines [24]. CCR5 expression by $CD4^+$ T cells was downregulated by ADSCs, which may be relevant to the biological processes indicated by the downregulated genes in hepatic inflammatory cells. Because CCR5 is a $CD4^+$ T-cell receptor that interacts with APCs, such as macrophages [25], suppression of CCR5 expression on $CD4^+$ T cells by ADSC might explain the amelioration of ConA-mediated hepatitis. Overall, the therapeutic efficacy of ADSCs impacted both $CD4^+$ and $CD11b^+$ cells in terms of alteration of levels of inflammatory humoral mediators and cytokine/chemokine profiles, thus contributing to amelioration of ConA-induced hepatitis.

A proportion of i.v. administered ADSCs were present in the livers of ConA mice injected with ADSCs at a time point at which the liver had already been infiltrated with $Gr\text{-}1^+$ and $CD11b^+$ cells, whereas no ADSCs were present in the livers of mice injected with ConA following immediate treatment with ADSCs. This indicates that a liver undergoing inflammation attracts administered ADSCs. The extent of inflammation required to recruit ADSCs should be clarified, as it has previously been reported that hepatitis occurring just 30 min after ConA injection results in recruitment of a substantial number of stem cells to the liver in the BALB/c ConA hepatitis model [15]. Given that the migratory capabilities of MSCs are well known although not yet fully investigated [26], how ADSCs are recruited to an already inflamed liver as a result of ConA administration should be examined. In addition, the ADSCs administered to C57BL/6 mice immediately after ConA injection resided in the lung. In spite of the fact that they were not detected in the liver, these ADSCs prevented ConA hepatitis, indicating the remote effect of ADSCs. Thus, indirect mediators produced by ADSCs associated with their anti-inflammatory effects should be investigated intensively.

◀ **Figure 4.** *Gene expression analysis in the liver of ConA-induced hepatitis mice treated with ADSCs.* C57BL/6 female mice were injected i.v. with 300 μg of ConA. (A, B, and E) Immediately or (C, D, and F) 3 h after ConA injection, mice were treated with 1×10^5 ADSCs via the tail vein ($n = 3$ each). Liver tissues were analyzed 2 h after ADSC administration and RNA was isolated for gene expression analysis using a DNA microarray. Data shown are from one experiment performed. (A, B) One-way clustering analysis (A) and principal component analysis (B) of the 589 differentially expressed genes in treated and untreated ConA-injected mice. (C, D) One-way clustering analysis (C) and principal component analysis (D) of the 309 differentially expressed genes in treated (after 3 h) and untreated ConA-injected mice followed. Colors indicate the intensity of gene upregulation (red), downregulation (green), and no change (black). (E, F) One-way clustering analysis of gene expression in hematopoietic and stem cells (GSE27787) for annotated genes among the 589 (E) and 309 (F) genes.

Table 1. Maps relevant to genes for which the expression was affected in the liver of ConA-injected mice followed by ADSC treatment at 3 h.

Maps	*p*-value
Tissue remodeling and wound repair	0.000001438
Inflammatory response	0.000003973
Mitogenic signaling	0.0001056
Vascular development (angiogenesis)	0.0002926
DNA damage response	0.0004529
Apoptosis	0.0008909
Cystic fibrosis disease	0.001402
Myogenesis regulation	0.001571
Cell differentiation	0.002173
Immune system response	0.003304

In conclusion, the therapeutic anti-inflammatory efficacy of ADSCs relied on suppression of myeloid-lineage and $CD4^+$ T cells in the ConA-induced C57BL/6 murine hepatitis model. The application of ADSC therapy to various inflammatory liver diseases can be further developed by studies of their immunomodulatory effects.

Materials and methods

Murine acute hepatitis induced by ConA injection and treatment with ADSCs

C57BL/6J female mice (10–12 weeks old, Charles River Laboratories Japan Inc., Yokohama, Japan) were injected i.v. with 300 μg of ConA (Sigma-Aldrich, St. Louis, MO, USA) dissolved in PBS. For $CD4^+$ T-cell or $CD8^+$ T-cell depletion, 200 μg of purified anti-CD4 antibody from the culture supernatant of GK1.5 cells (ATCC, Manassas, VA, USA), or purified anti-CD8 antibody from the culture supernatant of 2.43 cells (ATCC), was injected i.p. for two consecutive days before ConA injection. For depletion of monocyte-macrophage lineage cells, 2 mg of clodronate (Sigma-Aldrich), which was encapsulated in liposomes using the COATSOME-EL-01-N liposome formulation kit (Nihonyushi, Tokyo, Japan) [27], was injected via the tail vein 2 days before ConA injection. For the prevention or treatment experiment, 1×10^5 ADSCs were administered i.v. immediately or 3 h after ConA injection. In some cohorts, blood was obtained under anesthesia, and liver and lung tissues were collected after euthanizing mice at 6, 12, and 24 h after ConA injection. A portion of the liver tissue was homogenized and the enriched fraction of inflammatory cells was obtained by gradient centrifugation using Ficoll–Hypaque (Sigma-Aldrich). Our institutional review board approved the care and use of laboratory animals in all experiments.

Isolation and culture of ADSCs and primary hepatocytes

Inguinal adipose tissues were obtained from C57BL/6J male mice (10–12 weeks old, Charles River Laboratories Japan Inc.) or GFP-transgenic mice (male, 10–12 weeks old, gift from Prof. Okabe, Osaka University, Japan). Tissues were digested with 0.075% collagenase type I (Wako Pure Chemical Industries Ltd., Osaka, Japan), washed with PBS, and then transferred to a culture dish with DMEM/F-12 1:1 medium (Life Technologies–Invitrogen, Carlsbad, CA, USA) supplemented with 10% heat-inactivated FBS and 1% antibiotic–antimycotic solution (Life Technologies). Cells were maintained and expanded by eight to ten passages before use.

To obtain primary hepatocytes, C57BL/6J male mice (10–12 weeks old) were anesthetized by i.p. injection of pentobarbital (50 mg/kg; Kyoritsu Seiyaku, Tokyo, Japan) and injected with 10 mL of 0.75% type I collagenase solution via the portal vein. Liver tissues were minced to dissociate cells, filtered through a 100 μm mesh, and cultured in 10-cm culture dishes for 16 h until use.

Pluripotency of ADSCs

The pluripotency of ADSCs was examined using a mouse mesenchymal stem cell functional kit® (R&D Systems, Minneapolis, MN, USA), and immunohistochemical staining of cells that had differentiated into osteocytes, chondrocytes, and adipocytes was performed using anti-mouse ostepontin, anti-mouse collagen II, and anti-mouse FABP4 antibodies, respectively, in accordance with the manufacturer's instruction. Adipocyte differentiation was also assessed by staining using an aliquot of Oil Red O (WAKO).

Co-culture of ConA-stimulated hepatic inflammatory cells with ADSCs

Hepatic inflammatory cells were isolated from C57BL/6J female mice (10 weeks old) that had been injected i.v. with 300 μg of ConA 3 h before ($n = 4$). $CD4^+$ T cells and $CD11b^+$ cells were separated from the collected hepatic inflammatory cells using anti-CD4 and anti-CD11b magnetic beads (Miltenyi Biotec, Bergisch Gladbach, Germany). Then, 20 000 ADSCs were co-cultured with 4×10^5 of the isolated $CD4^+$ T cells or $CD11b^+$ cells in a 24-well plate (BD Falcon, San Jose, CA, USA) for 2 h ($n = 3$). After co-culture, floating cells were harvested, and RNA harvested using the MicroRNA isolation kit (Stratagene, La Jolla, CA, USA) for real-time PCR analysis to measure cytokine/chemokine gene expression.

Measurement of serum ALT and LDH activity

Blood was collected from the postorbital venous plexus and serum was separated from clotted blood after coagulation. The serum activity of ALT, and LDH was measured using L-type WAKO GPT J2, and LDH-J kits (Wako Pure Chemical Industries Ltd.), respectively, using autoanalytical equipment (Hitach7180, Hitachi Ltd., Tokyo, Japan), according to the manufacturer's protocol.

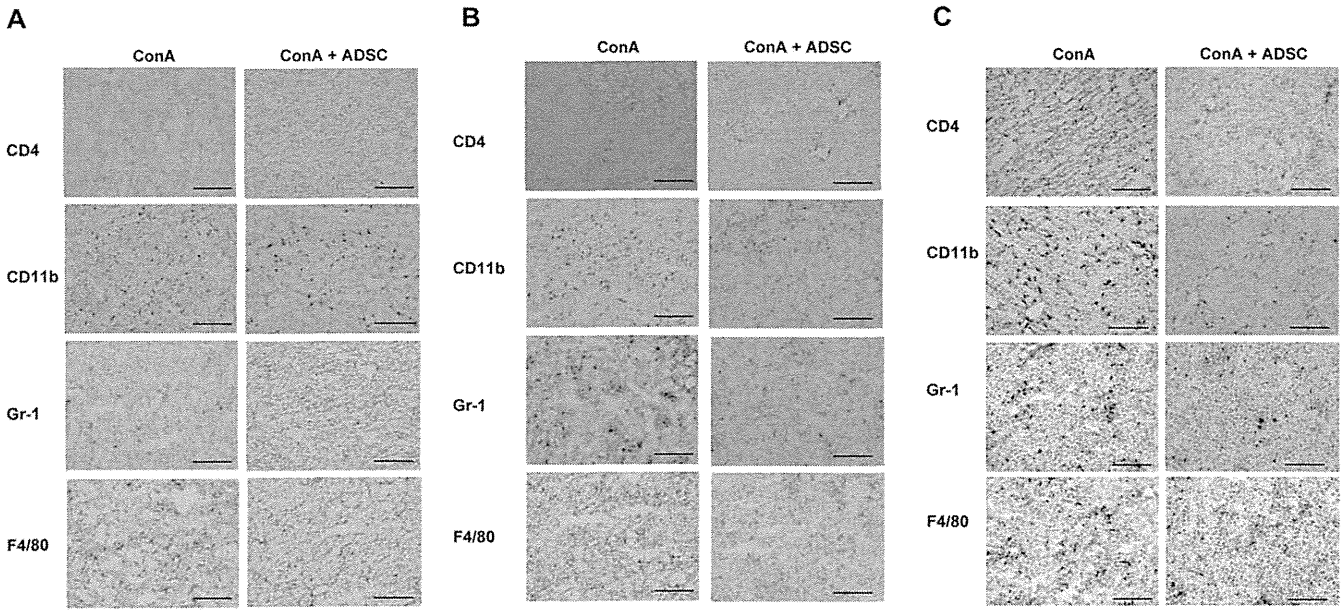

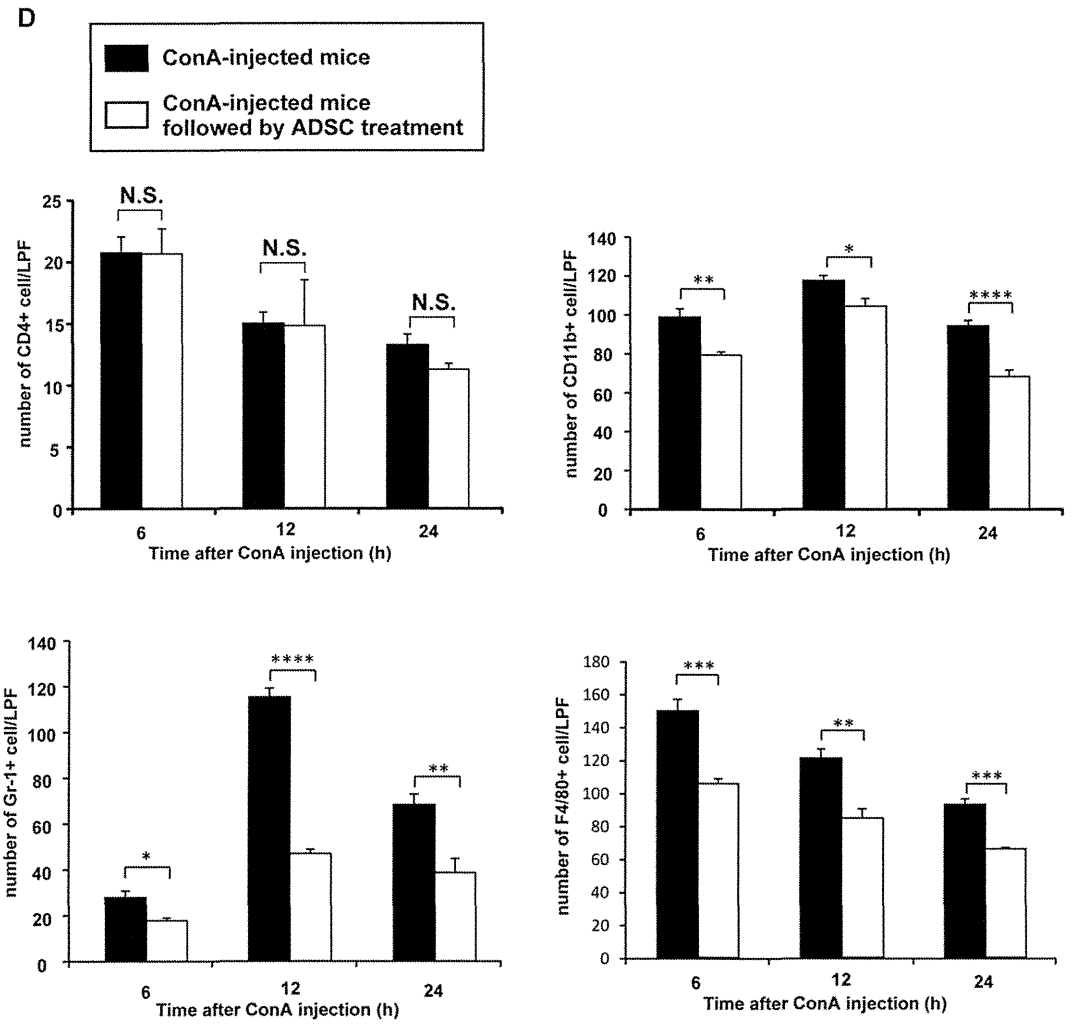

Measurement of serum cytokine/chemokine concentrations

Sera were obtained from ADSC-treated mice immediately or 3 h after ConA injection ($n = 3$ and $n = 4$, respectively), and from ConA-injected mice not treated with ADSCs ($n = 3$ and $n = 6$, respectively) at 6 h. Serum concentrations of cytokines and chemokines were measured using a Multiplex Bead Immunoassays kit, Mouse Cytokine 20-Plex Panel (Invitrogen, Carlsbad, CA, USA), following the manufacturer's protocol. The kit covers FGF-basic, GM-CSF, IFN-γ, IL-1α, IL-1β, IL-2, IL-4, IL-5, IL-6, IL-10, IL-12 (p40/p70), IL-13, IL-17, IP-10(CXCL10), KC, MCP-1, MIG(CXCL9), MIP-1α, TNF-α, and VEGF.

Histological and immunohistochemical analyses of liver and lung tissues

Harvested liver and lung tissues were fixed in 10% formaldehyde, embedded in paraffin, sectioned at 4 μm, and stained with H&E. For immunohistochemical analysis, the liver tissues were embedded in OCT compound (Sakura Finetek, Torrance, CA, USA), snap-frozen in liquid nitrogen, cryostat-sectioned, and fixed with methanol/acetone (1:1). The paraffin-embedded tissues were also sliced into 4 μm sections, mounted on microscope slides, and deparaffinized, followed by epitope retrieval using proteinase K (Dako, Glostrup, Denmark). The slides were incubated with peroxidase blocking reagent (Dako) for 15 min at room temperature to inhibit endogenous peroxidase activity, followed by incubation with protein blocking reagent (Dako) to avoid nonspecific protein reactions. The slides were incubated with primary antibodies (anti-mouse CD4, CD11b, Gr-1, F4/80) (BD Pharmingen, San Diego, CA, USA) and anti-GFP (MBL, Nagoya, Japan) diluted with PBS containing 1% BSA overnight at 4°C. After washing in PBS, the slides were then incubated with secondary antibodies (anti-rat, anti-rabbit; Nichirei, Japan) for 30 min at room temperature. The immune complexes were visualized using EnVision kits /HRP (DAB; Dako) followed by counterstaining with hematoxylin. The numbers of positive cells in each section were counted in four randomly selected fields at 100× magnification under a microscope.

RNA isolation and gene expression analysis by DNA microarray

Total RNA was obtained from the tissues or hepatic inflammatory cells in RNAlater (Ambion) using RNA isolation kit (Sigma-Aldrich) in accordance with the supplied protocol with slight modifications. Isolated RNA was amplified and labeled with the Cy3 using the Quick Amp labeling kit (Agilent Technologies, Santa Clara, CA, USA) in accordance with the manufacturer's protocol. cRNA of 1.65 μg was hybridized onto a Whole Mouse Genome 4 × 44K Array (Agilent Technologies) and scanned using a DNA Microarray Scanner (model G2505B, Agilent Technologies).

Gene expression data were analyzed using the GeneSpring analysis software (Agilent Technologies). Each measurement was divided by the 75th percentile of all measurements in that sample at per chip normalization. Hierarchical clustering and principal component analysis of gene expression was performed. Welch's *t*-test, with Benjamini and Hochberg's false discovery rate, was used to identify genes that were differentially expressed in the groups of interest. Analysis of biological processes was performed using the MetaCore software suite (GeneGo, Carlsbad, CA, USA). BRB array tools (http://linus.nci.nih.gov/BRB-ArrayTools.html) were also used for unsupervised or one-way clustering analyses. Microarray data were deposited in the NBCI Gene Expression Omnibus (GSE ID: GSE41465).

Flow cytometry

Cultured ADSCs were incubated in PBS supplemented with 2% BSA (Sigma-Aldrich) containing antibodies labeled with FITC or PE anti-mouse CD44 or CD90 (Beckman Coulter, Brea, CA, USA), and CD105 (Miltenyi Biotec) antibodies. Hepatic inflammatory cells isolated from mice were incubated with a mixture of FITC-labeled anti-mouse CD204 (AbD Serotec, Raleigh, NC, USA), PE-labeled anti-mouse Gr-1 (Miltenyi Biotec), and allophycocyanin-labeled anti-mouse CD11b (BioLegend, San Diego, CA, USA), or FITC-labeled anti-mouse CD11b (Beckman Coulter), PE-labeled anti-mouse Ly-6G (BioLegend), and allophycocyanin labeled anti-mouse Ly-6C (BioLegend) antibodies. The fluorescence intensity of the cells was measured using a FACSCalibur™ (Becton Dickinson, San Jose, CA, USA). Data obtained were visualized and analyzed using the FlowJo software (Tomy Digital Biology Co., Ltd., Tokyo, Japan).

Isolation of $CD11b^+Gr\text{-}1^+$ hepatic inflammatory cells and T-cell [3H]-thymidine incorporation assay

C57BL/6J female mice were injected with 300 μg of ConA and then injected with 1×10^5 ADSCs after 3 h ($n = 3$). Three

◀ **Figure 5.** Immunohistochemical analysis of inflammatory cells in the liver of ConA-induced hepatitis mice treated with ADSCs. (A–C) Immunohistochemical staining of the liver. C57BL/6 female mice were injected i.v. with 300 μg of ConA. Then, 3 h later, the mice were injected with ADSCs via the tail vein. Liver tissues were obtained at (A) 6, (B)12, or (C) 24 h after ConA injection ($n = 4$ per each time point). Immunohistochemical staining was conducted using anti-CD4, anti-CD11b, anti-Gr-1, and anti-F4/80 antibodies. Stained liver images shown are representative of three experiments performed. Magnification: ×100. Bars: 200 μm. (D) Quantification of $CD4^+$, $CD11b^+$, $Gr\text{-}1^+$, and $F4/80^+$ cells in four visual fields per ×100 low-power field in the liver of representative mice from each group. Data are shown as mean +SE ($n = 4$) and are representative of three experiments performed. $^*p < 0.05$, $^{**}p < 0.01$, $^{***}p < 0.005$, $^{****}p < 0.001$; Student's *t*-test. n.s.: not significant.

hours later, hepatic inflammatory cells were isolated and incubated with FITC-labeled anti-mouse CD11b (Beckman Coulter) and PE-labeled anti-mouse Gr-1 (Miltenyi Biotec) antibodies. The $CD11b^+Gr\text{-}1^+$ population was collected using a FACSAira II™ (Becton Dickinson). $CD11b^+Gr\text{-}1^+$ cells (1×10^5), which had been irradiated with 2000 rads, were co-cultured with 1×10^5 purified splenic T cells isolated from C57BL/6J mice in RPMI1640 medium (Invitrogen) supplemented with 10% heat-inactivated FBS, 1% antibiotic–antimycotic solution (Life Technologies), and ConA (4 μg/mL) for 48 h ($n = 4$). The culture was pulsed with [3H]thymidine (1 μCi/well) for 16 h and harvested. Thymidine incorporation was measured using a beta-counter (PerkinElmer, Waltham, MA, USA).

NO assay

C57BL/6J female mice were injected with 300 μg of ConA. Three hours later, 1×10^5 ADSCs were injected via the tail vein. After a further 3 h, hepatic inflammatory cells were isolated from ConA hepatitis mice with or without ADSC treatment ($n = 3$ each) and incubated in PBS supplemented with 2% BSA, PE-labeled anti-mouse Gr-1 antibody, and allophycocyanin-labeled anti-mouse CD11b antibody. Cells were then incubated in PBS containing 2.5 mg/mL diaminofluorescein-FM diacetate (Sekisui Medical Co., Ltd., Tokyo, Japan), which emits fluorescence at 515 nm in a reaction with NO, at 37°C for 30 min and subjected to FACS analysis using a FACSCalibur flow cytometer.

Arginase assay

Female C57BL/6J mice were injected with 300 μg of ConA. Three hours later, 1×10^5 ADSCs were injected via the tail vein. After further 3 h, hepatic inflammatory cells were isolated from ConA hepatitis mice with or without ADSC treatment ($n = 3$ each) and were lysed with PBS containing 10 mM Tris-HCl (pH 7.4) and 0.4% Triton X-100, supplemented with the proteinase inhibitor cocktail, cOmplete, Mini, EDTA-free® (Roche, Basel, Switzerland). One hundred micrograms of the lysis aliquot obtained were subject to an arginase activity assay using a QuantiChrom™ Arginase Assay kit (BioAssay Systems, Hayward, CA), which measures urea produced from the substrate, in accordance with the manufacturer's protocol.

Statistical analysis

All data are expressed as means ± SE. Statistical analyses were performed using the JMP software (ver.9.02; SAS Institute Japan Inc., Tokyo, Japan). Student's *t*-test and Wilcoxon signed-rank test were used. p values < 0.05 were considered to indicate statistical significance.

Acknowledgements: This study was supported, in part, by subsidies from the Japanese Ministry of Education, Culture, Sports, Science, and Technology and the Japanese Ministry of Health, Labor, and Welfare.

Conflict of interest: The authors declare no financial or commercial conflict of interest.

References

1 **Zuk, P. A., Zhu, M., Ashjian, P., De Ugarte, D. A., Huang, J. I., Mizuno, H., Alfonso, Z. C. et al.**, Human adipose tissue is a source of multipotent stem cells. *Mol. Biol. Cell* 2002. **13**: 4279–4295.

2 **Chamberlain, G., Fox, J., Ashton, B. and Middleton, J.**, Concise review: mesenchymal stem cells: their phenotype, differentiation capacity, immunological features, and potential for homing. *Stem Cells* 2007. **25**: 2739–2749.

3 **Perez-Cano, R., Vranckx, J. J., Lasso, J. M., Calabrese, C., Merck, B., Milstein, A. M., Sassoon, E. et al.**, Prospective trial of adipose-derived regenerative cell (ADRC)-enriched fat grafting for partial mastectomy defects: the RESTORE-2 trial. *Eur. J. Surg. Oncol.* 2012. **38**: 382–389.

4 **Janssens, S.**, Stem cells in the treatment of heart disease. *Annu. Rev. Med.* 2010. **61**: 287–300.

5 **Hoogduijn, M. J., Popp, F., Verbeek, R., Masoodi, M., Nicolaou, A., Baan, C. and Dahlke, M. H.**, The immunomodulatory properties of mesenchymal stem cells and their use for immunotherapy. *Int. Immunopharmacol.* 2010. **10**: 1496–1500.

6 **Baroni, G. S., Pastorelli, A., Manzin, A., Benedetti, A., Marucci, L., Solforosi, L., Di Sario, A. et al.**, Hepatic stellate cell activation and liver fibrosis are associated with necroinflammatory injury and Th1-like response in chronic hepatitis C. *Liver* 1999. **19**: 212–219.

7 **Cerny, A. and Chisari, F. V.**, Pathogenesis of chronic hepatitis C: immunological features of hepatic injury and viral persistence. *Hepatology* 1999. **30**: 595–601.

8 **Gershwin, M. E., Ansari, A. A., Mackay, I. R., Nakanuma, Y., Nishio, A., Rowley, M. J. and Coppel, R. L.**, Primary biliary cirrhosis: an orchestrated immune response against epithelial cells. *Immunol. Rev.* 2000. **174**: 210–225.

9 **Krawitt, E. L.**, Autoimmune hepatitis. *N. Engl. J. Med.* 1996. **334**: 897–903.

10 **Fujii, H. and Kawada, N.**, Inflammation and fibrogenesis in steatohepatitis. *J. Gastroenterol.* 2012. **47**: 215–225.

11 **Dienes, H. P. and Drebber, U.**, Pathology of immune-mediated liver injury. *Dig. Dis.* 2010. **28**: 57–62.

12 **Dai, L. J., Li, H. Y., Guan, L. X., Ritchie, G. and Zhou, J. X.**, The therapeutic potential of bone marrow-derived mesenchymal stem cells on hepatic cirrhosis. *Stem Cell Res.* 2009. **2**: 16–25.

13 **Sanders, D. A., Moothoo, D. N., Raftery, J., Howard, A. J., Helliwell, J. R. and Naismith, J. H.**, The 1.2 A resolution structure of the Con A-dimannose complex. *J. Mol. Biol.* 2001. **310**: 875–884.

14 **Kato, M., Ikeda, N., Matsushita, E., Kaneko, S. and Kobayashi, K.**, Involvement of IL-10, an anti-inflammatory cytokine in murine liver injury induced by concanavalin A. *Hepatol. Res.* 2001. **20**: 232–243.

15 **Kubo, N., Narumi, S., Kijima, H., Mizukami, H., Yagihashi, S., Hakamada, K. and Nakane, A.**, Efficacy of adipose tissue-derived mesenchymal stem cells for fulminant hepatitis in mice induced by concanavalin A. *J. Gastroenterol. Hepatol.* 2012. **27**: 165–172.

16 **Murdoch, C., Muthana, M., Coffelt, S. B. and Lewis, C. E.**, The role of myeloid cells in the promotion of tumour angiogenesis. *Nat. Rev. Cancer* 2008. **8**: 618–631.

17 **Banas, A., Teratani, T., Yamamoto, Y., Tokuhara, M., Takeshita, F., Quinn, G., Okochi, H. et al.**, Adipose tissue-derived mesenchymal stem cells as a source of human hepatocytes. *Hepatology* 2007. **46**: 219–228.

18 **Kaneko, Y., Harada, M., Kawano, T., Yamashita, M., Shibata, Y., Gejyo, F., Nakayama, T. et al.**, Augmentation of Valpha14 NKT cell-mediated cytotoxicity by interleukin 4 in an autocrine mechanism resulting in the development of concanavalin A-induced hepatitis. *J. Exp. Med.* 2000. **191**: 105–114.

19 **Tiegs, G., Hentschel, J. and Wendel, A.**, A T cell-dependent experimental liver injury in mice inducible by concanavalin A. *J. Clin. Invest.* 1992. **90**: 196–203.

20 **Halder, R. C., Aguilera, C., Maricic, I. and Kumar, V.**, Type II NKT cell-mediated anergy induction in type I NKT cells prevents inflammatory liver disease. *J. Clin. Invest.* 2007. **117**: 2302–2312.

21 **Schwabe, R. F. and Brenner, D. A.**, Mechanisms of liver injury. I. TNF-alpha-induced liver injury: role of IKK, JNK, and ROS pathways. *Am. J. Physiol. Gastrointest. Liver Physiol.* 2006. **290**: G583–G589.

22 **Schumann, J., Wolf, D., Pahl, A., Brune, K., Papadopoulos, T., van Rooijen, N. and Tiegs, G.**, Importance of Kupffer cells for T-cell-dependent liver injury in mice. *Am. J. Pathol.* 2000. **157**: 1671–1683.

23 **Clegg, C. H., Rulffes, J. T., Wallace, P. M. and Haugen, H. S.**, Regulation of an extrathymic T-cell development pathway by oncostatin M. *Nature* 1996. **384**: 261–263.

24 **Constant, S. L. and Bottomly, K.**, Induction of Th1 and Th2 CD4+ T cell responses: the alternative approaches. *Annu. Rev. Immunol.* 1997. **15**: 297–322.

25 **Contento, R. L., Molon, B., Boularan, C., Pozzan, T., Manes, S., Marullo, S. and Viola, A.**, CXCR4-CCR5: a couple modulating T cell functions. *Proc. Natl. Acad. Sci. USA* 2008. **105**: 10101–10106.

26 **Ponte, A. L., Marais, E., Gallay, N., Langonne, A., Delorme, B., Herault, O., Charbord, P. et al.**, The in vitro migration capacity of human bone marrow mesenchymal stem cells: comparison of chemokine and growth factor chemotactic activities. *Stem Cells* 2007. **25**: 1737–1745.

27 **Kushiyama, T., Oda, T., Yamada, M., Higashi, K., Yamamoto, K., Oshima, N., Sakurai, Y. et al.**, Effects of liposome-encapsulated clodronate on chlorhexidine gluconate-induced peritoneal fibrosis in rats. *Nephrol. Dial. Transplant.* 2011. **26**: 3143–3154.

Abbreviations: **ADSC**: adipose tissue derived stromal stem cell · **ALT**: alanine transferase · **LDH**: lactate dehydrogenase · **MDSC**: myeloid-derived suppressor cell · **MSC**: mesenchymal stromal stem cell

Full correspondence: Dr. Shuichi Kaneko, Disease Control and Homeostasis, Kanazawa University, 13-1 Takara-machi, Kanazawa, Ishikawa 920-8641, Japan
Fax: +81-76-234-4250
e-mail: skaneko@m-kanazwa.jp

Received: 17/3/2013
Revised: 3/7/2013
Accepted: 6/8/2013
Accepted article online: 12/8/2013

Evaluation of eligibility criteria in living donor liver transplantation for hepatocellular carcinoma by α-SMA-positive cancer-associated fibroblasts

HIROYUKI TAKAMURA[1], SHINICHI NAKANUMA[1], HIRONORI HAYASHI[1], HIDEHIRO TAJIMA[1], KAHEITA KAKINOKI[2], SEISYO SAKAI[1], ISAMU MAKINO[1], HISATOSHI NAKAGAWARA[1], TOMOHARU MIYASHITA[1], KOICHI OKAMOTO[1], KEISHI NAKAMURA[1], KATUNOBU OYAMA[1], MASASHI INOKUCHI[1], ITASU NINOMIYA[1], HIROHISA KITAGAWA[1], SACHIO FUSHIDA[1], TAKASHI FUJIMURA[1], ICHIRO OHNISHI[1], MASATO KAYAHARA[1], TAKASHI TANI[1], KUNIAKI ARAI[2], TARO YAMASHITA[2], TATSUYA YAMASHITA[2], HOSHIKO KITAMURA[3], HIROKO IKEDA[3,4], SHUICHI KANEKO[2], YASUNI NAKANUMA[3], OSAMU MATSUI[5] and TETSUO OHTA[1]

Departments of [1]Gastroenterologic Surgery, [2]Gastroenterology, [3]Diagnostic Pathology, [4]Human Pathology and [5]Radiology, Graduate School of Medicine, Kanazawa University, Kanazawa, Ishikawa 920-8641, Japan

Received March 21, 2013; Accepted June 7, 2013

DOI: 10.3892/or.2013.2616

Abstract. The eligibility criteria of liver transplantation (LT) for hepatocellular carcinoma (HCC) must clearly confirm the prognosis not only from pathological diagnosis but also from pre-operative imaging diagnosis. In the present study, we evaluated published eligibility criteria for LT based on both pre-operative imaging diagnosis and pathological diagnosis using living donor liver transplantation (LDLT) recipients at our hospital by α-smooth muscle actin (SMA)-positive cancer-associated fibroblasts (CAFs) in HCC. The Up-to-seven (Up-to-7), Asan and Tokyo criteria were evaluated, in both overall survival and HCC disease-free survival, to be statistically significantly beneficial criteria to define post-LDLT prognosis. Recipients only within Up-to-7 criteria based on both pre-operative imaging diagnosis and pathological diagnosis survived without HCC recurrence. Recipients with proliferation of α-SMA-positive CAFs in HCC had significantly poorer prognosis. All survival recipients without HCC recurrence, who were above the Up-to-7 criteria in pathological diagnosis, had no proliferation of α-SMA-positive CAFs. As a result of multivariate analysis, the significant independent factors defining prognosis of recipients after LDLT for HCC were Up-to-7 criteria and proliferation of α-SMA-positive CAFs. The ideal eligibility criteria for LDLT with HCC is Up-to-7 criteria and α-SMA-positive CAFs was considered to be an important factor in HCC recurrence. LDLT should be limited to recipients within Up-to-7 criteria or without proliferation of α-SMA-positive CAFs.

Correspondence to: Dr Hiroyuki Takamura, Department of Gastroenterologic Surgery, Kanazawa University, 13-1 Takaramachi, Kanazawa, Ishikawa 920-8641, Japan
E-mail: takamuh@staff.kanazawa-u.ac.jp

Abbreviations: AFP, α-fetoprotein; CAFs, cancer-associated fibroblasts; CTAP, computer tomography under angiography during arterial portography; CTHA, computer tomography under angiography during hepatic arteriography; DCP, des-γ-carboxyprothrombin; DDLT, deceased donor liver transplantation; HCC, hepatocellular carcinoma; DFS, disease-free survival; dynamic MDCT, dynamic multi-detectable-row computer tomography; Gd-EOB-DTPA-MRI, gadolinium ethoxybenzyl diethylenetriamine pentaacetic acid-enhanced magnetic resonance imaging; HBV, hepatitis B virus; HCV, hepatitis C virus; LC, liver cirrhosis; LDLT, living donor liver transplantation; LT, liver transplantation; OS, overall survival; RFA, radiofrequency ablation therapy; TACL, transarterial chemolipiodolisation; Up-to-7, Up-to-seven criteria

Key words: living donor liver transplantation, hepatocellular carcinoma, cancer-associated fibroblast, Up-to-seven criteria, α-smooth muscle actin

Introduction

In 1996, eligibility criteria such as the Milan criteria (MC) of liver transplantation (LT) for hepatocellular carcinoma (HCC) were reported by Mazzaferro *et al* (1). MC emphasized LT as a therapeutic option for patients with HCC. Living donor liver transplantation (LDLT) is virtually the only option for patients with HCC in the east Asian countries such as Korea (2) or Japan (3-9), where the number of deceased donors is limited, and for patients above MC in western countries such as the United States and in Europe. Therefore, understanding how far the criteria of LT for HCC can be extended in LDLT from MC is key in improving the outcomes in regions with limited organ donors. There have been several reports of expanded criteria as indications of LT for HCC, such as the Up-to-seven (Up-to-7) criteria (10),

University California of San Francisco (UCSF) criteria (11), Asan criteria (2), Tokyo (5-5 rule) criteria (3), Kyoto criteria (4,5) and Kyushu criteria (6-8). In addition, Kyoto criteria (4,5) and Kyushu criteria (6-8) showed pre-operative tumor markers such as the des-γ-carboxyprothrombin (DCP) level. In the present study, we evaluated the predictive values of the previously proposed selection criteria, including Up-to 7 criteria, UCSF criteria, Asan criteria, Tokyo criteria, Kyoto criteria and Kyushu criteria, on the overall survival (OS) and HCC disease-free survival (DFS) of LDLT recipients with HCC. These criteria are categorized into several types which are based only on pre-operative imaging diagnosis, or on pathological diagnosis of the explant liver, which consider microvascular invasion as above criteria, and take account of tumor markers. According to Japanese national data (9), in addition to the MC, it is reported that the values of tumor markers [α-fetoprotein (AFP) and DCP] define prognosis, but as various factors are involved in tumor markers, it is difficult to incorporate them into international eligibility criteria of LT for HCC. Regardless of whether it is deceased donor liver transplantation (DDLT) or LDLT, the criteria of LT for HCC should be defined solely by simple factors such as tumor diameter or number to guarantee their international applicability. Furthermore, eligibility criteria of LT for HCC must significantly define the prognosis for recipients in evaluations which are based not only on pathological diagnosis of the explant liver, but also on pre-operative imaging diagnosis. However, it is important to perform pre-operative imaging diagnosis of HCC close to post-operative pathological diagnosis. If the accuracy of imaging diagnosis of HCC is low, the reliability of the criteria decreases, therefore, pre-operative imaging diagnosis should be performed accurately using some imaging diagnostic modalities. In order to enhance imaging diagnostic accuracy for HCC, in addition to dynamic multi-detectable-row computer tomography (dynamic MDCT) and gadolinium ethoxybenzyl diethylenetriamine pentaacetic acid-enhanced magnetic resonance imaging (Gd-EOB-DTPA-MRI) (12,13), we also obtained images as far as possible using CT under angiography [during arterial portography (CTAP) and during hepatic arteriography (CTHA)] (14-17). In view of the fact that a healthy living donor is exposed to major risks by hepatectomy, recurrence of HCC after LT in the recipient must be avoided. To receive LDLT under Japanese health insurance, although no restrictions are imposed as to therapeutic history 3 months prior to LT, the recipient must satisfy the MC in the pre-operative final imaging diagnosis. Eligibility criteria have been reported by various high-volume centers in Japan (3-8) and there are attempts to widen eligibility of LDLT for HCC under health insurance. In this context, in order to expand the eligibility criteria from within MC, we evaluated which criteria were the most suitable from the two viewpoints of pre-operative imaging diagnosis and pathological diagnosis with recipients who had performed precise pre-operative diagnostic imaging and had been observed for >5 years after LDLT for HCC. Furthermore, we evaluated the appropriateness of the above criteria from the viewpoint of proliferation of α-smooth muscle actin (SMA)-positive cancer-associated fibroblasts (CAFs), which are strongly related to cancer progression and invasion (18,19). However, there are no reports which evaluate HCC recurrence after LT from the viewpoint of α-SMA-positive CAFs. We therefore evaluated the relationship between HCC recurrence after LDLT and proliferation of α-SMA-positive CAFs, as well as the correlation between eligibility criteria and α-SMA-positive CAFs.

Materials and methods

Patients. From July 2003 to December 2007, 22 consecutive LDLTs for liver cirrhosis (LC) with HCC were performed at Kanazawa University Hospital (Ishikawa, Japan) after receiving approval from the Ethics and Indications Committee of Kanazawa University. Our selection criteria for the patients with HCC were as follows: no modality except LDLT available to cure patients with HCC and end-stage liver disease, no extrahepatic metastasis and no macrovascular invasion such as portal vein or hepatic vein infiltrations. We limited adaptation of LDLT for HCC to within MC under health insurance of Japan since January 2008, but performed LDLT for above MC recipients by own expenses until December 2007. Therefore targeted cases for the present study were limited to recipients who had undergone LDLT by December 2007. Twenty-two patients had HCC, proven histologically. The median age of the 22 patients was 55.5 years (range, 47-64 years). Written informed consent for the present study was obtained from each patient. In addition, the study was approved by the Kanazawa University Ethics Committee. Tumor-specific evaluations, including abdominal and thoracic dynamic MDCT, abdominal CTAP, abdominal CTHA, abdominal Gd-EOB-DTPA-MRI, bone scintigraphy, and the determination of AFP and DCP (Protein induced by Vitamin K, PIVKA-II), were performed for all LDLT candidates. The diameter and number of HCCs were determined by multiple radiologists, based on pre-operative imaging studies within one month of LT. Thus, the variables used in the criteria, including tumor diameter and number, were based on these data. The explants were examined histologically. For pathological examination, whole liver explants were fixed in 10% formalin and cut into 5-mm slices to facilitate gross and histological examinations. Following macroscopic examination, the nodular lesions were embedded in paraffin, cut into 4-inch sections and stained with hematoxylin and eosin. The incidence of microvascular invasion and histological grades were subsequently estimated within these criteria. Microvascular invasion was defined as microscopic portal vein or hepatic vein invasion of cancer cells. The stage was determined for each patient according to the AJCC/UICC (6th edition) guidelines (20) and UNOS TMN (21). Among the 22 patients, 10 (45.5%) met the MC according to pre-operative first imaging diagnosis, while 12 did not. According to previous studies, Up-to 7, UCSF, Asan, Tokyo, Kyoto and Kyushu criteria were applied and the predictive impacts of these criteria for HCC recurrence were evaluated by univariate analyses. The previously proposed selection criteria for HCC are briefly described below and are shown in Table I. The Up-to-7 criteria are defined as HCC with seven as the sum of the diameter of the largest tumor (in cm) and the number of tumors. The UCSF criteria are defined as HCC meeting the following criteria: solitary tumor of ≤6.5 cm, or ≤3 nodules with the largest lesion of ≤4.5 cm and a total tumor diameter of ≤8 cm. The Asan criteria are defined as HCC meeting the following criteria: tumor up to

Table I. Summary of published outcomes of liver transplantation for HCC between recipients satisfying expanded/extended eligibility criteria.

Eligibility criteria name and definition	Authors, year (ref.)	Study design and staging method	Tumor characteristics	Cases (n)	OS (%) 1-year	OS (%) 3-year	OS (%) 5-year	DFS (%) 1-year	DFS (%) 3-year	DFS (%) 5-year
UCSF criteria: no extrahepatic spread or macrovascular invasion. Solitary tumor with diameter ≤65 mm, or ≤3 nodules with maximum diameter ≤45 mm and total tumor diameter ≤80 mm.	Yao *et al*, 2001 (11)	Retrospective analysis. Staging: explant pathology	Within UCSF criteria and above MC	60	90		75.2			
			Above UCSF	10	50	20	-			
Up-to-7 criteria: no extrahepatic disease or microvascular invasion. Sum of number of nodules and diameter of largest nodule (cm) ≤7	Mazzoferro *et al*, 2001 (10)	Retrospective analysis. Staging: explant pathology	Within Up-to-7 criteria and above MC without microvasular invasion	283		77.7	71.2			
			Within Up-to-7 criteria and above MC with microvasular invasion	116		60.2	47.4			
			Within MC without microvascular invasion	361		81.8	76.1			
			Within MC with microvascular invasion	44		77.1	71.6			
			Above Up-to-7 criteria and without microvasular invasion	333		71.8	64			
			Above Up-to-7 criteria with microvasular invasion	338		41.7	33			
Asan criteria: no extrahepatic disease or macrovascular invasion. ≤6 nodules with maximum diameter 50 mm.	Lee *et al*, 2008 (2)	Retrospective analysis. Staging: explant pathology	Within Asan criteria and above MC	22	100	88.9	80			
			Within MC	152	86.6	79.2	76			
			Beyond Asan criteria	32	65.7	34.1	18.9			
Tokyo criteria (5-5): No extrahepatic disease or macrovascular invasion. ≤5 nodules with maximum diameter 50 mm.	Sugawara *et al*, 2007 (3)	Analysis against predefined criteria. Staging: pre-LDLT radiology (imaging).	Within Tokyo criteria	72				97	94	
			Above Tokyo criteria	6				50	50	
Kyoto criteria: no extrahepatic disease or macrovascular invasion. ≤10 nodules with maximum diameter 50 mm. PIVKA-II ≤400 mAU/ml.	Ito *et al*, 2007 (4)	Retrospective analysis. Staging: explant pathology.	Within Kyoto criteria	78			86.7			
			Above Kyoto criteria	40			34.4			
	Takada *et al*, 2007 (5)	Retrospective analysis. Staging: pre-LDLT radiology (imaging).	Within Kyoto criteria	83			87			
			Above Kyoto criteria	44			37			
Kyushu criteria: no extrahepatic disease or macrovascular invasion. Any nodules with maximum diameter 50 mm. PIVKA-II ≤300 mAU/ml.	Shirabe *et al*, 2011 (8)	Retrospective analysis. Staging: pre-LDLT radiology (imaging).	Within Kyushu criteria and above MC	48				85	80	80
			Above Kyushu criteria	6				16.7	0	0

HCC, hepatocellular carcinoma; OS, post-operative overall survival rate of recipient; DFS, post-operative HCC disease-free survival rate of recipient; Up-to-7, Up-to-seven criteria; LDLT, living donor liver transplantation; MC, Milan criteria.

6 nodules with a maximum diameter of 5 cm without gross vascular invasion. The Tokyo criteria are defined as HCC meeting the following criteria: tumor of up to 5 nodules with a maximum diameter of 5 cm (5-5 rule) that are evaluated with pre-operative imaging. The Kyoto criteria are defined as HCC meeting the following criteria: ≤10 tumors that are all ≤5 cm in diameter and DCP of ≤400 mAU/ml. The Kyushu University criteria are defined as HCC with tumor diameter <5 cm or DCP <300 mAU/ml. In the 7 above MC recipients who underwent pre-LDLT therapy to downstage HCC, transarterial chemo-lipiodolisation (TACL) was performed in all cases, and radiofrequency ablation therapy (RFA) was also performed in 2 cases. The recipients who underwent pre-LDLT therapy for HCC were observed for ≥3 months from the end of the pre-operative therapy to LDLT. There were 4 out of 5 recipients who were downstaged from above MC (pre-operative first imaging diagnosis) to within MC (pre-operative final imaging diagnosis) by pre-LDLT therapy. In the 15 cases were LDLT was performed without prior therapy, the pre-operative first imaging diagnosis was considered the pre-operative final imaging diagnosis. There were 13 cases in total that received therapy for HCC in the past before LDLT; TACL had been performed in 11 cases and several treatments in 10 cases. RFA had been performed in 8 cases, percutaneous ethanol injection therapy (PEIT) in 5 cases and hepatectomy in 2 cases. In addition, transarterial infusion chemotherapy had been performed in only 1 case. The clinical follow-up of patients after LDLT for HCC followed a strict protocol, which did not change during the study period. The patients were seen biweekly for the first 6 months and then monthly. The patients underwent enhanced MDCT or Gd-EOB-DTPA-MRI at 4-6 month intervals. Liver biopsy, hepatic angiography with CT, bone scintigraphy or 2-Fluoro 2-deoxyglucose positron emission tomography (FDG-PET) CT was also performed if deterioration in the graft function or a rise in the AFP or DCP levels was noted. The mean follow-up period was 7 years.

Immunohistochemistry. The proliferation of α-SMA-positive CAFs was evaluated immunohistologically. When several tumors were present, the tumor with microvascular invasion was evaluated. If no microvascular invasion was found, tumors which had the poorer histological degree of differentiation or differentiated into biliary tract type (CK7-positive or CK19-positive), were evaluated. Tumor specimens were fixed in 10% formalin and embedded in paraffin. The expressions of α-SMA in HCC were examined immunohistochemically using respective primary antibodies using EnVision+ System (DAKO). De-waxed 4-μm sections were incubated with 1:50 with protein blocking serum for 10 min to block non-specific binding and immunostaining was performed using EnVision+ System. Briefly, the slides were incubated with each primary antibody (1:50) at 4˚C overnight. After washing, the EnVision+ polymer solution was applied for 1 h. The reaction products were visualized via a diaminobenzidine (DAB) reaction. The specimens were then lightly counterstained with hematoxylin and examined under a fluorescence microscope. Primary antibody used for immunostaining was Actin α2 Smooth Muscle rabbit anti-human polyclonal antibody (Novus Biologicals, Littleton, CO, USA).

Computer-assisted image analysis (19). We used computer-assisted image analysis to quantify the value of α-SMA expression in HCC. After staining for α-SMA, the histological sections were observed using a microscope equipped with a charge coupled-device color camera (Olympus Co., Japan) under constant electrical and optical conditions. A random selection of 10 fields in most poorly differentiated and α-SMA-positive CAF proliferating lesions of HCC were assessed for α-SMA expression. Using an imaging processor (VH Analyzer; Keyence Co., Japan) the percentage of α-SMA expression stromal area was quantified as the relative percentage of the α-SMA-positive stromal area to the selected fields of cancer.

Statistical analysis. All statistical analyses were performed using SPSS Software v20 (IBM-Japan, Tokyo, Japan). The continuous variables were compared using the Mann-Whitney U test. All variables are expressed as means ± standard deviation (SD). The categorical data were compared using χ^2 tests. We compared Kaplan-Meier distributions of time to mortality or HCC recurrence after LDLT with the log-rank test or generalized Wilcoxon. Cox's proportional hazard model was used to identify independent variables for post-operative recurrence of HCC. The comparative evaluation was performed among the Milan, Up-to-7, Asan, Tokyo, Kyoto, Kyushu criteria, degree of α-SMA-positive CAFs and clinicopathological variables including pre-operative serum AFP levels and serum DPC levels, presence of microvascular invasion, histological grade of the tumor (poorly differentiated), the number of tumors and maximum diameter of tumor on the resected specimen. The differences were considered statistically significant when the P-value was <0.05.

Results

Table II shows background characteristics of 22 recipients who underwent LDLT for HCC according to post-LDLT with or without HCC recurrence. The average age of recipients was 56 years, 17 of whom were males, and the average MELD score of recipients was 14 points. There were 12 recipients with hepatitis C viral (HCV) hepatitis and 10 recipients with hepatitis B viral (HBV) hepatitis. Seventeen recipients were given right hepatic graft and 5 recipients were given left hepatic graft with caudate lobe. The average graft volume/standard liver volume ratio (GV/SLV) (22) of recipients was 46%. The average age of the donors was 36 years. There were 5 cases with acute cellular rejection (ACR) after LDLT (23%). No operation-related mortality of recipients occurred. All donors returned to society promptly after the donor operation. For immunosuppressive drugs, tacrolimus (FK) was used in 17 cases (77.3%) and cyclosporine (CyA) was used in 5 cases. Administration of steroids (prednisone) was limited to 1 week after LDLT in 11 cases (50%), while in the remaining 11 cases administration was continued for a longer period of ≥6 months post-operatively. Mycophenolate mofetil (MMF) was also used in 13 cases (59%). As to UNOS TNM, 2 cases were stage I, 4 cases were stage II and 16 cases (73%) were stage IV. Regarding UICC TNM, 2 cases were stage I, 18 cases (82%) were stage II and 2 cases were stage III. Concerning histological differentiation of HCC, well-differentiated HCC was only one case, moderately differentiated HCC were 15 cases

Table II. Background characteristics of recipients who underwent LDLT for HCC according to post-LDLT with or without HCC recurrence.

Factor	All recipients (22 cases)	Recipients without post-LDLT HCC recurrence (13 cases)	Recipients with post-LDLT HCC recurrence (9 cases)
Age, years (mean ± SD)	56±4 (range 47-64)	56±4	55±3
MELD score (mean ± SD)	14±8 (range 1-30)	15±9	11±7
GV/SLV (mean ± SD)	46.3±7.0 (range 36-60)	46.1±7.5	46.6±7.2
Donor age (mean ± SD)	36±12 (range 20-61)	38±13	35±12
AFP (ng/ml) (mean ± SD)	148±264	169±323	118±182
DCP (mAU/l) (mean ± SD)	183±388	85±179	323±573
Gender (female/male)	5/17	5/ 8	0/9
HCV/HBV	12/10	7/ 6	5/4
LDLT graft (Left/Right)	5/17	2/11	3/6
Post-LDLT complication, n (%)			
Bile duct stenosis	6 (27)	4 (31)	2 (22)
CMV infection	9 (41)	6 (46)	3 (33)
ACR	5 (23)	2 (15)	3 (33)
Immunosuppressant			
CNI (FK/CyA)	17/5	10/3	7/2
Prednisolone, n (%)	11 (50)	8 (62)	3 (33)
MMF, n (%)	13 (59)	8 (62)	5 (56)
Child-Pugh, n (%)			
A	4 (18)	1 (8)	3 (33)
B	12 (55)	8 (61)	12 (55)
C	6 (27)	4 (31)	6 (27)
UNOS TNM, n (%)			
I,II	6 (28)	6 (46)	0
IV	16 (72)	7 (54)	9 (100)[a]
UICC TNM, n (%)			
I	2 (9)	2 (15)	0
II	18 (82)	10 (77)	8 (89)
III	2 (9)	1 (8)	1 (11)
Histological grade (poorly and combined), n (%)	6 (27.2)	4 (31)	2 (22)
Microvascular invasion, n (%)	16 (73)	9 (69)	7 (78)
Bile duct invasion, n (%)	1 (5)	1 (8)	0
Intrahepatic metastasis, n (%)	11 (50)	5 (39)	6 (67)
SVR, n (%)	14 (64)	7 (54)	7 (78)
Pre-LDLT treatment for HCC, n (%)	15 (68)	9 (69)	6 (67)

[a]P<0.05 in the comparison of the with and without post-LDLT HCC recurrence groups using χ^2 test (analysis was considered statistically significant). LDLT, living donor liver transplantation; HCC, hepatocellular carcinoma; GV/SLV, actual graft volume/recipient standard liver volume ratio; AFP, α-fetoprotein; DCP, des-γ-carboxyprothrombin; CMV, cytomegalovirus; ACR, acute cellular rejection; CNI, calcineurin inhibitor; HCV, hepatitis C viral hepatitis; HBV, hepatitis B viral hepatitis; MMF, mycophenolate mofetil; SVR, sustained viral responder for hepatitis C or B virus; SD, standard deviation.

(68%) which accounted for the majority, poorly differentiated HCC were 3 cases and the combined type were 3 cases. In the statistical study, well and moderately differentiated were both considered as differentiated type, while poorly and combined were both considered as poorly differentiated type. There were 13 recipients (59%) who had received prior therapy for HCC and 7 recipients who had received pre-LT therapy to downstage HCC. A total of 15 cases (68%) had a history of prior therapy or had received pre-operative therapy for HCC prior to LDLT. In the 7 cases where pre-LT therapy was performed to downstage HCC, 4 cases were downstaged from above MC to within MC. However, in 2 of these 4 cases where downstaging of HCC was attempted, recurrence of HCC was found after LT. To date, 8 recipients have died. The cause of mortality was HCC recurrence in 6 cases, accounting for the majority, liver failure due to recurrence of HCV hepatitis in 1 case and cancer in another organ (oropharyngeal carcinoma) in 1 case, but in all 8 cases, recurrence of HCC was found. HCC recurrence in post-LT recipients was found most often in graft liver, but lung metastasis, bone metastasis, adrenal metastasis and peritoneal dissemination or lymph node metastasis were also observed concurrently. There were no operation-related deaths in the recipients. As shown in Table II, a significant correlation of HCC recurrence after LT was found only with UNOS TNM.

As shown in Fig. 1A and C, all cases judged as within Up-to-7 criteria in the pre-operative first imaging diagnosis

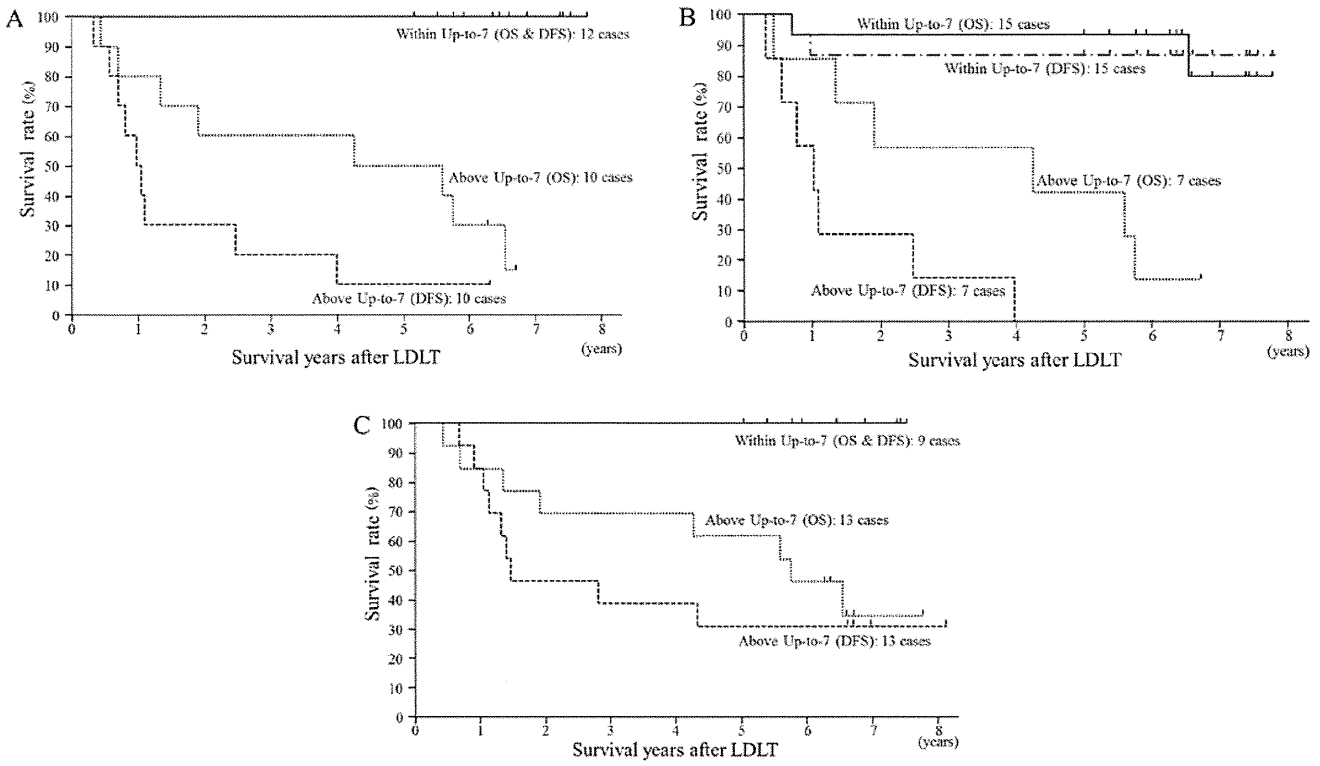

Figure 1. (A) Overall survival (OS) and hepatocellular carcinoma (HCC) disease-free survival (DFS) in living donor liver transplantation (LDLT) patients with HCC according to Up-to-seven (Up-to-7) criteria (permitting microvascular invasion) which were determined by pre-operative first imaging diagnosis. All 12 cases within Up-to-7 criteria survived without HCC recurrence. The OS and the DFS survival rates of within Up-to-7 criteria are statistically significantly ($P<0.001$) better than above Up-to-7 criteria. (B) OS and DFS in LDLT patients with HCC according to Up-to-7 criteria (permitting microvascular invasion) which were determined by final imaging diagnosis. There were only 2 recurrence cases in 18 cases within Up-to-7 criteria. The OS and the DFS of within Up-to-7 criteria are statistically significantly ($P<0.001$) better than above Up-to-7 criteria. (C) OS and DFS in LDLT patients with HCC according to Up-to-7 criteria (permitting microvascular invasion) which were determined by pathological diagnosis. All 9 cases within Up-to-7 criteria survived without HCC recurrence. The OS and the DFS of within the Up-to-7 criteria are statistically significantly ($P<0.05$) better than above the Up-to-7 criteria.

or pathological diagnosis survived without HCC recurrence. On the other hand, in cases judged as above Up-to-7 criteria in the pre-operative first imaging diagnosis and pathological diagnosis, the 5-year DFS was 10 and 21%, respectively, which is poor prognosis. Fig. 1B shows the OS and DFS of recipients based on the Up-to-7 criteria evaluated by pre-operative final imaging diagnosis. Comparing OS and DFS of within Up-to-7 criteria with above criteria, a significant difference was found, and there were 2 cases of recurrence in within Up-to-7 criteria.

Table III shows the OS and DFS of recipients according to the MC, Up-to-7, Asan, Tokyo, Kyoto and Kyushu criteria based on the pre-operative first imaging diagnosis and pathological diagnosis. Recipients within Asan criteria which permit wider eligibility than Up-to-7 or UCSF criteria had a significantly better prognosis than above criteria, but there were 2 cases of HCC recurrence among the within criteria in pre-operative first imaging diagnosis. The Tokyo criteria gave the same results as the Asan criteria. According to the Asan criteria or Tokyo criteria, two deaths due to HCC recurrence were confirmed based on the pre-operative first imaging diagnosis, thus regarding eligibility for LDLT, the Up-to-7 criteria were deemed the most appropriate criteria. On the other hand, according to the Kyoto criteria, in an evaluation based on pre-operative final imaging diagnosis, there was a significant correlation with the prognosis of recipients, but in an evaluation based on the pathological diagnosis, the prognosis was not reflected. According to the Kyushu criteria, a significant difference was found in DFS between within criteria and above criteria, but for OS, there was no significant difference. These two criteria appear useful to distinguish patients at very high risk of HCC recurrence in a single high-volume center, but in the current situation where it is not possible to prevent recurrence and no particularly effective therapy after HCC recurrence, they cannot be considered universal standard criteria. The most appropriate criteria which define the prognosis of recipients after LDLT for HCC, for both pre-operative imaging diagnosis and pathological diagnosis, are the Up-to-7 criteria, and in view of the burden of living donors, it should be made the global standard of eligibility criteria for LT in HCC.

As shown in Table IV, the degree of histological differentiation of HCC, the values of serum AFP and serum DCP, and the presence of microvascular invasion were not significantly correlated with the prognosis after LDLT. In other words, microvascular invasion should be admitted as within criteria.

Proliferation of α-SMA-positive CAFs which is thought to be strongly related to cancer progression and invasion, clearly specifies the prognosis after LDLT in HCC. However, α-SMA was not found to be expressed in HCC cancer cells. We categorized the proliferation of α-SMA-positive CAF into the following 3 groups.

Group I (Fig. 2A), 10 cases: low grade proliferation of α-SMA-positive CAFs; proliferation of cancer stroma not

Table III. Outcome of recipients of LDLT for HCC according to published eligibility criteria and α-SMA-positive CAF in HCC.

Eligibility criteria name	Staging method	Classification	Cases (n)	OS (%)				P-value	DFS (%)				P-value
				1-year	3-year	5-year	7-year		1-year	3-year	5-year	7-year	
Milan criteria (1)	Pre-operative first	Within criteria	10	10 (100%)	10 (100%)	10 (100%)	4 (100%)	<0.005	10 (100%)	10 (100%)	10 (100%)	4 (100%)	<0.001
	imaging diagnosis	Above criteria	12	10 (83%)	8 (67%)	7 (58%)	-		7 (58%)	4 (33%)	3 (25%)	-	
	Pre-operative final	Within criteria	14	13 (93%)	13 (93%)	13 (93%)	4 (77%)	<0.005	12 (86%)	12 (86%)	12 (86%)	4 (86%)	<0.001
	imaging diagnosis	Above criteria	8	7 (88%)	5 (63%)	4 (50%)	-		5 (63%)	2 (25%)	1 (13%)	0	
	Pathological diagnosis	Within criteria	7	7 (100%)	7 (100%)	7 (100%)	4 (100%)	<0.05	7 (100%)	7 (100%)	7 (100%)	4 (100%)	<0.05
		Above criteria	15	13 (87%)	11 (73%)	10 (67%)	1 (40%)		10 (67%)	7 (47%)	6 (40%)	1 (40%)	
Up-to-7 criteria (10)	Pre-operative first	Within criteria	12	12 (100%)	12 (100%)	12 (100%)	4 (100%)	<0.0005	12 (100%)	12 (100%)	12 (100%)	4 (100%)	<0.00001
	imaging diagnosis	Above criteria	10	8 (80%)	6 (60%)	5 (50%)	-		5 (50%)	2 (20%)	1 (10%)	-	
	Pre-operative final	Within criteria	15	14 (93%)	14 (93%)	14 (93%)	4 (80%)	<0.0005	13 (87%)	13 (87%)	13 (87%)	4 (87%)	<0.00005
	imaging diagnosis	Above criteria	7	6 (86%)	4 (57%)	3 (43%)	-		4 (57%)	1 (14%)	0	0	
	Pathological diagnosis	Within criteria	9	9 (100%)	9 (100%)	9 (100%)	3 (100%)	<0.01	9 (100%)	9 (100%)	9 (100%)	3 (100%)	<0.005
		Above criteria	13	11 (85%)	9 (69%)	8 (62%)	1 (35%)		6 (55%)	3 (27%)	2 (21%)	-	
Asan criteria (2)	Pre-operative first	Within criteria	14	13 (93%)	13 (93%)	13 (93%)	4 (80%)	<0.005	12 (86%)	12 (86%)	12 (86%)	4 (86%)	<0.005
	imaging diagnosis	Above criteria	8	7 (88%)	5 (63%)	4 (50%)	-		5 (63%)	2 (25%)	1 (13%)	-	
	Pre-operative final	Within criteria	15	14 (93%)	14 (93%)	14 (93%)	4 (80%)	<0.0005	13 (88%)	13 (88%)	13 (88%)	4 (88%)	<0.00005
	imaging diagnosis	Above criteria	7	6 (71%)	4 (57%)	3 (43%)	-		4 (57%)	1 (14%)	0	0	
	Pathological diagnosis	Within criteria	13	12 (92%)	12 (92%)	12 (92%)	4 (79%)	<0.05	11 (85%)	11 (85%)	11 (85%)	4 (85%)	<0.005
		Above criteria	9	8 (89%)	6 (67%)	5 (56%)	-		6 (67%)	3 (33%)	2 (22%)	-	
Tokyo criteria	Pre-operative first	Within criteria	14	14 (100%)	14 (100%)	13 (93%)	4 (79%)	<0.005	13 (93%)	13 (93%)	11 (86%)	4 (86%)	<00001
(5-5 rule) (3)	imaging diagnosis	Above criteria	8	6 (75%)	4 (50%)	3 (38%)	-		4 (50%)	1 (13%)	1 (13%)	-	
	Pre-operative final	Within criteria	16	15 (94%)	15 (94%)	15 (94%)	4 (74%)	<0.005	14 (88%)	14 (88%)	13 (81%)	4 (81%)	<0.00001
	imaging diagnosis	Above criteria	6	5 (83%)	3 (50%)	2 (33%)	-		3 (50%)	0	0	0	
	Pathological diagnosis	Within criteria	11	11 (100%)	11 (100%)	11 (100%)	4 (100%)	<0.005	11 (100%)	11 (100%)	11 (100%)	4 (100%)	<0.00001
		Above criteria	11	9 (82%)	7 (64%)	6 (55%)	-		6 (55%)	3 (27%)	2 (21%)	-	
Kyoto criteria (4,5)	Pre-operative first	Within criteria	16	15 (94%)	14 (88%)	14 (88%)	4 (69%)	**>0.05**	13 (81%)	13 (81%)	12 (75%)	4 (75%)	<0.01
	imaging diagnosis	Above criteria	6	5 (83%)	4 (67%)	3 (33%)	-		4 (67%)	1 (17%)	1 (17%)	-	
	Pre-operative final	Within criteria	17	16 (94%)	15 (88%)	15 (88%)	4 (70%)	<0.05	14 (82%)	14 (82%)	13 (76%)	4 (76%)	<0.005
	imaging diagnosis	Above criteria	5	4 (80%)	3 (60%)	2 (40%)	-		3 (60%)	0	0	0	
	Pathological diagnosis	Within criteria	16	15 (94%)	14 (88%)	14 (88%)	4 (63%)	**>0.1**	13 (81%)	12 (75%)	11 (69%)	4 (69%)	**>0.1**
		Above criteria	6	5 (83%)	4 (67%)	3 (50%)	-		4 (67%)	2 (33%)	2 (33%)	-	

Table III. Continued.

Eligibility criteria name	Staging method	Classification	Cases (n)	OS (%)						DFS (%)					
				1-year	3-year	5-year	7-year	P-value		1-year	3-year	5-year	7-year	P-value	
Kyushu criteria (6-8)	Pre-operative first	Within criteria	18	17 (94%)	15 (83%)	14 (78%)	4 (61%)	**>0.5**		15 (83%)	13 (72%)	12 (67%)	4 (67%)	<0.05	
	imaging diagnosis	Above criteria	4	3 (75%)	3 (75%)	3 (75%)	-			2 (50%)	1 (25%)	1 (25%)	-		
	Pre-operative final	Within criteria	18	17 (94%)	15 (83%)	14 (78%)	4 (61%)	**>0.5**		15 (83%)	13 (72%)	12 (67%)	4 (67%)	<0.05	
	imaging diagnosis	Above criteria	4	3 (75%)	3 (75%)	3 (75%)	-			2 (50%)	1 (25%)	1 (25%)	-		
	Pathological diagnosis	Within criteria	18	17 (89%)	15 (83%)	14 (78%)	4 (61%)	**>0.5**		15 (83%)	13 (72%)	12 (67%)	4 (67%)	<0.05	
		Above criteria	4	3 (25%)	3 (25%)	3 (25%)	-			2 (50%)	1 (25%)	1 (25%)	-		
α-SMA-positive CAF	Pathological diagnosis	Grade I	10	10 (100%)	10 (100%)	10 (100%)	3 (88%)	<0.0001		10 (100%)	10 (100%)	9 (90%)	3 (90%)	<0.00001	
		Grade II	8	8 (100%)	7 (88%)	6 (75%)	1 (60%)			7 (88%)	4 (50%)	4 (50%)	1 (50%)		
		Grade III	4	2 (50%)	1 (25%)	1 (25%)	0			0	0	0	0		

Survival rates were estimated using the Kaplan-Meier method and compared between groups by the log-rank and generalized Wilcoxon analysis. P<0.05, analysis was considered statistically significant; P≥0.05, analysis was not considered statistically significant. LDLT, living donor liver transplantation; HCC, hepatocellular carcinoma; α-SMA, α-smooth muscle actin; CAF, cancer-associated fibroblast; OS, post-operative overall survival rate of recipient; DFS, post-operative HCC disease-free survival rate of recipient.

Figure 2. Representative immunohistochemical staining for α-smooth muscle actin (α-SMA) in hepatocellular carcinoma (HCC) tissue sections of living donor liver transplantation (LDLT) patients. (A) α-SMA positivity in cancer-associated fibroblasts (CAFs) of HCC is low grade (<1.0%). (B) α-SMA positivity in CAF of HCC is middle grade (<10%). (C) α-SMA positivity in CAF of HCC is high grade (≥10%).

found, only slight proliferation of α-SMA-positive CAFs and staining was <1% of ten fields under high power view.

Group II (Fig. 2B), 8 cases: middle grade proliferation of α-SMA-positive CAFs; cancer nests were bordered over their whole circumference by α-SMA-positive CAFs, but the cancer stroma (CAFs) accounted for <10% of ten fields under high power view.

Table IV. Correlation between α-SMA-positive CAF in HCC of LDLT recipients with clinicopathological factors and published eligibility criteria.

Factor	All redipients (22 cases)	α-SMA-positive CAF	
		Grade I (10 cases)	Grade II, III (12 cases)
Age, years (mean ± SD)	56±4	56±3	55±4
Gender (female/male)	5/17	5/5	0/12[a]
MELD score (mean ± SD)	14±8 (range 1-30)	15±9	11±7
HCV/HBV	12/10	5/5	7/5
Child-Pugh, n (%)			
A	4 (18)	0	4 (33)[a]
B, C	12 (55)	10 (100)	8 (67)[a]
Pre-LDLT treatment for HCC, n (%)	15 (68)	7 (70)	8 (67)
AFP (ng/ml) (mean ± SD)	148±264	53±87	227±343
DCP (mAU/l) (mean ± SD)	183±388	106±202	246±508
CEA (ng/ml) (mean ± SD)	4.4±1.5	4.4±1.7	4.5±1.3
CA19-9 (U/ml) (mean ± SD)	73.4±82.6	101.7±94.7	45.1±62.7
HCC numbers (pre-LDLT first imaging diagnosis) (mean ± SD)	5.3±5.8	2.2±2.3	7.8±6.7[b]
HCC numbers (pathological diagnosis) (mean ± SD)	6.6±6.0	4.0±3.3	8.8±7.0
HCC maximum diameter (pre-LDLT first imaging diagnosis) (mean ± SD) (cm)	2.2±1.6	1.4±1.4	2.9±1.5
HCC maximum diameter (pathological diagnosis) (cm)	2.9±1.2	2.5±1.2	3.2±1.1
Sum of all HCC diameters (pre-LDLT first imaging diagnosis) (mean ± SD) (cm)	7.6±10.1	2.0±3.8	12.2±11.9[b]
Sum of all HCC diameters (pathological diagnosis) (mean ± SD) (cm)	10.3±9.4	6.6±5.9	13.4±10.8
UNOS TNM, n (%)			
I, II	6 (28)	5 (50)	1 (8)[a]
IV	16 (72)	5 (50)	11 (92)[a]
Histological grade (poorly and combined), n (%)	6 (27.2)	2 (20)	4 (33)
Microvascular invasion, n (%)	16 (73)	7 (70)	9 (75)
Intrahepatic metastasis, n (%)	11 (50)	5 (50)	6 (50)
Post-LDLT HCC recurrence, n (%)	9 (41)	1 (10)	8 (67)[a]
Recipient mortality, n (%)	8 (36)	1 (10)	7 (53)[a]
Above Milan criteria, n (%)			
Imaging	12 (55)	3 (25)	9 (75)[a]
Pathology	15 (68)	5 (33)	10 (67)
Above Up-to-7 criteria, n (%)			
Imaging	10 (46)	2 (20)	8 (80)[a]
Pathology	13 (59)	4 (31)	9 (69)
Above Asan criteria, n (%)			
Imaging	8 (36)	2 (25)	6 (75)
Pathology	9 (41)	3 (33)	6 (67)
Above Tokyo criteria, n (%)			
Imaging	8 (36)	1 (13)	7 (87)[a]
Pathology	11 (50)	3 (27)	8 (73)
Above Kyoto criteria, n (%)			
Imaging	6 (27)	1 (17)	5 (83)
Pathology	6 (27)	2 (33)	4 (67)
Above Kyushu criteria, n (%)			
Imaging	4 (18)	1 (25)	3 (75)
Pathology	4 (18)	1 (25)	3 (75)

[a]$P<0.05$ in the comparison of the with and without proliferation of α-SMA-positive CAF groups using χ^2 tests (analysis was considered statistically significant). [b]$P<0.05$ in the comparison of the with and without proliferation of α-SMA-positive CAF groups using the Mann-Whitney U test (analysis was considered statistically significant). α-SMA, α-smooth muscle actin; CAF, cancer-associated fibroblast; HCC, hepatocellular carcinoma; LDLT, living donor liver transplantation; AFP, α-fetoprotein; DCP, des-γ-carboxyprothrombin; HCV, hepatitis C viral hepatitis; HBV, hepatitis B viral hepatitis; SVR, sustained viral responder for hepatitis C or B virus; SD, standard deviation; imaging, HCC in the explanted liver was evaluated by pre-operative first imaging diagnosis; pathology, HCC in the explanted liver was evaluated by post-operative pathological diagnosis.